THE AMERICAN MINERALOGIST, VOL. 52, SEPTEMBER-OCTOBER, 1967

A SERPENTINE MINERAL SHOWING DIVERSE STRAIN-RELIEF MECHANISMS

F. AUMENTO, *Geological Survey of Canada, Ottawa, Ontario, Canada*

ABSTRACT

An unstable serpentine polymorph which exhibits the combined properties characteristic of a number of other known polymorphs is described. Macrocrystals of the mineral, from the Tilly Foster Mine, New York State, indicate that it is a six-layered monoclinic serpentine, with each successive layer displaced relative to its neighbours by $\pm a/3$ and $\pm b/3$ and, or, by a rotation of $\pm 60°$. Individual layers are further modulated periodically in the a crystal direction. The resulting crystal has superlattice controlled a and c parameters.

Finer fractions of a powdered macrocrystal, observed by electron microscopy, show that it tends to break down into smaller, simpler units: thin corrugated plates are formed, which themselves part along weak corrugation joints, forming elongated rods. The formation of rods deprives the basic serpentine layers of the satisfactory strain relief mechanism attributed to corrugation. The rods are seen to compensate for this deprivation by curling parallel to their elongation, eventually producing more stable chrysotile-like tubes. The complete metamorphosis from plates to tubes has been followed by selected area electron diffraction.

INTRODUCTION

During a systematic study of the serpentine minerals, an olive-green, platy mineral, labelled "Serpentine Pseudocrystals", was discovered amongst the specimens of the National Mineral Collection of Canada. The mineral is part of a hand specimen collected from the Tilly Foster Mine, Brewster, Putnam County, New York State. It is closely associated with magnesite, chondrodite, magnetite and chlorite. However, sufficient quantities of the mineral, free from magnetite and other impurities, could be selected without difficulty for chemical analysis.

MORPHOLOGY AND OPTICAL DATA

The mineral exhibits a strong platy habit, with a perfect cleavage parallel to (001). Flakes, ranging in size up to 5 mm across, can be bent with ease. Two other good cleavages, parallel to (100) and (010), give the crystals a euhedral appearance, which, although generally platy, at times can approximate a cube. The density, determined with a Berman balance, is 2.45 ± 0.01 gm/cc.

Polysynthetic twinning parallel to (001) is apparent under the polarizing microscope. The twinning, together with the morphology and optical orientations, is shown in Figure (1). The refractive indices determined by the double variation method, were found to vary from plate to plate. Plates parallel to (001) extinguish at 7°–10° to the edges, and give a centered biaxial interference figure. The biaxial angle, determined for a number of plates with a universal stage, is also variable. Optical properties

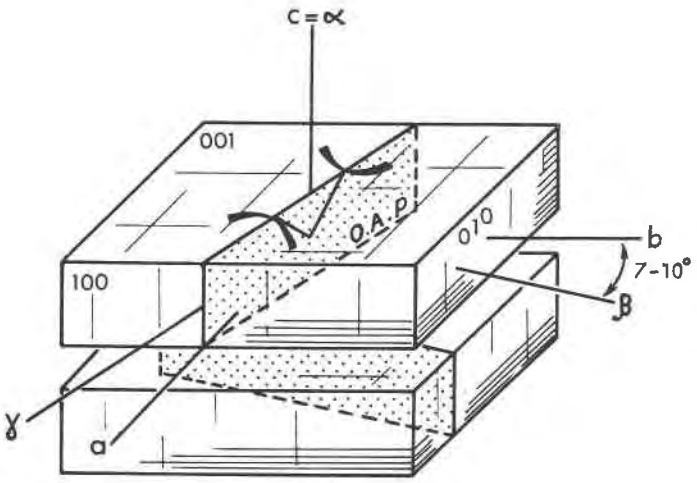

FIG. 1. Morphology, optical orientations, and twin relationships of the new serpentine mineral.

of the serpentine mineral are given below with refractive indices for sodium light.

$\alpha = 1.520-1.526$, $\beta = 1.522-1.528$, $\gamma = 1.528-1.535$, $2V = 83°–90°$, Sign = −Ve, Elong.: Fast or slow.

Chemical Analysis

A composite analysis of the mineral from classical wet chemical and spectrographic analyses by J. L. Bouvier follows:

SiO_2 41.70, TiO_2 0.07, Al_2O_3 0.31, Fe_2O_3+FeO 2.43, Cr_2O_3 0.002, B_2O_3 0.010, MgO 40.83, MnO 0.035, CaO 0.16, BaO 0.010, K_2O 0.04, P_2O_5 0.03, H_2O^+ 13.19, H_2O^- 1.45, Total 100.27%. NiO, Na_2O, V_2O_5, SO_3 and CO_2 were not detected.

Thermal Analyses

Three DTA curves are given in Figure 2. The first curve (2A) is that of a sample heated at a rate of +8°C/min. up to 1260°C. For the second (2B), equal amounts of the residue from the first run were mixed with fresh sample and then run at the same heating rate to 1480°C. The third (2C) is that of a sample previously treated for one hour with 1 N hydrochloric acid at 95°C.

The dynamic thermogravimetric analyses (TGA) (2E) were recorded at the same heating rate, whilst for the static TGA curve (2F) the sample was maintained at each steady temperature for twelve hours before recording the weight.

The residues of each of the thermal analysis samples were examined

by X-ray powder diffraction. Samples heated to 760°C and 900°C gave identical powder patterns, showing poorly crystallized forsterite. The composition of this synthesized forsterite could be calculated from the diffraction patterns (after Jambor and Smith (1964)) to be 97.6 percent Fo. Samples heated to between 1150°C and 1405°C showed two well crystallized phases: the major one was identified as protoenstatite, the minor one as forsterite. On heating to 1480°C the forsterite pattern intensified while the protoenstatite lines grew much fainter. The sample treated with hydrochloric acid was amorphous to X rays both before and after heating to 1040°C.

X-ray Powder Diffraction

Debye-Scherrer, counter diffractometric, and Guinier focusing techniques were used in an attempt to resolve all possible reflections and to determine accurate cell parameters. The counter diffractometer proved

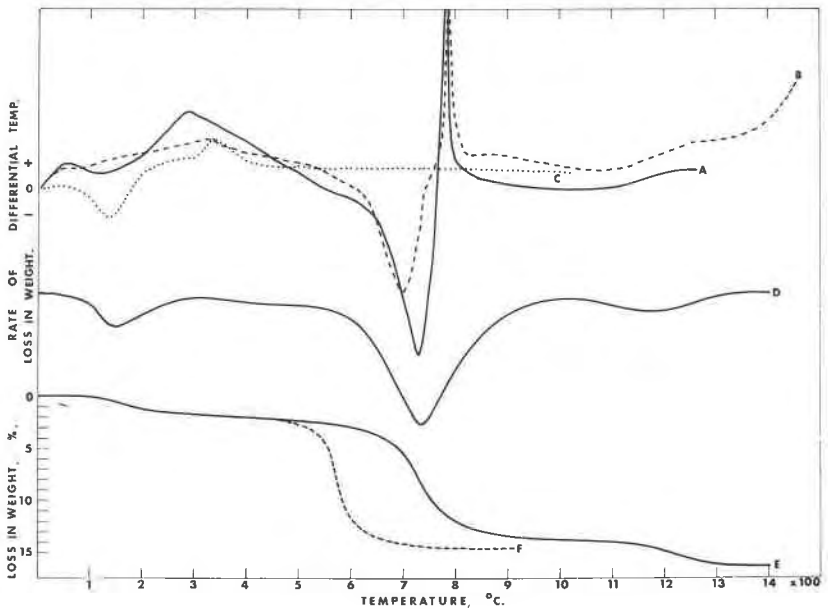

FIG. 2. Thermal analyses of the new serpentine mineral. Heating rate (for curves A to E) of +8°C/minute.

A. DTA. of fresh sample.
B. DTA. of 50 percent residue from *A* plus 50 percent of fresh sample.
C. DTA. of sample previously treated with 1 N HCl for one hour at 95°C.
D. DTG. curve.
E. Dynamic TGA curve.
F. Static TGA curve.

TABLE 1. STEP-SCANNED DIFFRACTOGRAM OF THE SERPENTINE MINERAL AT 25°C.

No.	I_{100}	$d_{obs.}$	hkl	$\frac{nh}{nl}$	$d_{calc.}$
1	100	7.363	001		7.265
2	23	4.548	020		4.611
3	5	4.41	—	3	4.370
4	5	4.09	—	5	4.020
5	53	3.639	002		3.632
6	12	2.657	130		2.660
7	13	2.586	200		2.655
8	15	2.507	$13\bar{1}$		2.521
9	19	2.477	131		2.475
10	11	2.089	132		2.117
11	16	1.8205	004		1.816
12	9	1.7421	150		1.742
13	10	1.5372	060		1.537
14	8	1.4555	005		1.453
15	6	1.307	$33\bar{3}$		1.326
16	6	1.212	006		1.211
17	5	1.105			
18	5	1.007			
19	5	.962			
20	5	.913			

Recorded with Ni-filtered Cu radiation and a quartz internal standard. The lines are indexed on the basic cell dimensions $a=5.32$, $b=9.22$, $c=7.28$ Å, $\beta=93.3°$. Superlattice indices based on multiples (n) of a or c are also given for weak lines at 4.41 and 4.09 Å.

to be best suited to the problem. The diffractogram (table 1) shows a combination of spacings and intensities similar to those of clino-chrysotile, with the addition of a few weak lines. Debye-Scherrer photographs had indicated the possible existence of weak lines on the higher 2θ angle side of the broad (020) peak (as shown by superlattice reflections of antigorite and ortho-serpentines). The region from 5 Å to 2.5 Å was therefore repeatedly step-scanned with the diffractometer: two very weak lines, at 4.41 and 4.09 Å, were resolved from an area of high background on the higher 2θ angle side of peak (020). No other faint lines could be resolved, although the high uneven background associated with these lines may have been due to a superimposition of a number of weak lines. The pattern, with the exception of the two weak lines mentioned, was indexed using the cell parameters and indexed reflections recorded by precession photography (next section). More precise cell parameters were then calculated from the indexed diffractogram, giving a monoclinic cell with the following parameters:-$a=5.320\pm0.005$, $b=9.222\pm$

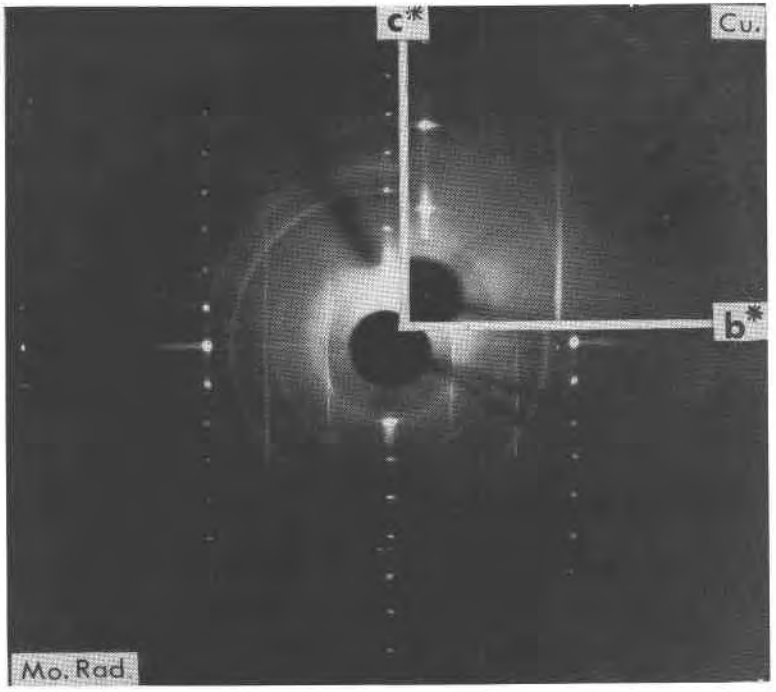

FIG. 3. Zero-level b^* c^* precession photograph of new serpentine. Note continuous streaks parallel to c^* when $k \neq 0$ or $6n$.

0.005, $c = 7.277 \pm 0.005$ Å $\beta = 93.3° \pm 0.5°$. However, a multiple parameter is required if the additional weak lines at 4.41 and 4.09 Å are to be indexed. Ambiguities as to which parameter is the multiple (the a parameter as in antigorite, or the c parameter as in the ortho-serpentines) can be partially resolved from single crystal X-ray and electron diffraction photography.

A sample treated with 1 N hydrochloric acid at 95°C for one hour gave an amorphous diffraction pattern, as is attributed to chrysotiles.

SINGLE CRYSTAL X-RAY DIFFRACTION

A combination of precession and Weissenberg photography, using both Cu and Mo radiation, permitted the recording of up to six levels about the a^*, b^* and c^* axes.

Composites of the zero levels a^* c^* and b^* c^*, taken with the precession camera, are given in Figures (3) and (4).

The following conditions for systematic reflections, based on the basic unit cell with $a = 5.32$ Å and $c = 7.28$ Å, are apparent:

hkl : $h + k = 2n$

$0kl$: $k = 2n$

$h0l$: $h = 2n$

$hk0$: $h + k = 2n$

$h00$: $h = 2n$

$0k0$: $k = 2n$

$00l$: no conditions

Three space groups, namely Cm, $C2$ or $C2/m$, are therefore possible for this serpentine polymorph.

Two very striking features are immediately apparent in the single crystal photographs: (1) All reflections recorded show multiple spots parallel to the a^* axis clustered about eight-fold multiple values of h. The clusters are interrupted along layer-lines, and are never made up of more than five spots. Taking all the multiple spots separately, the a

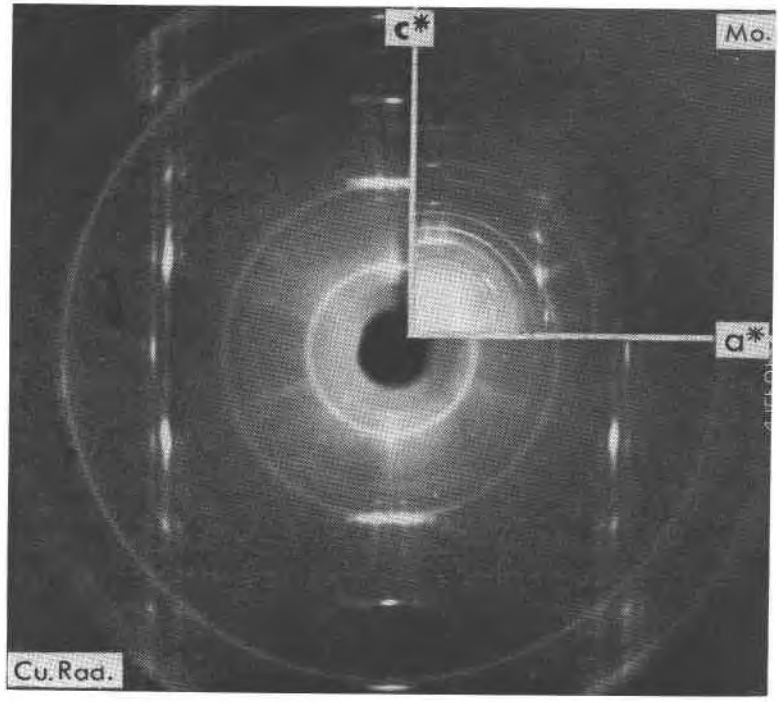

FIG. 4. Zero-level a^* c^* precession photograph of new serpentine. Note superlattice controlled clustering of spots parallel to a^* and elongation of spots parallel to c^* when $h \neq 0$.

parameter has a value of 41.5 Å ($=5.32\times8$), the value required to index all the lines of the powder diffractogram. As in antigorite, the clustering of reflections around certain multiple values of h could be taken to represent a typical superlattice effect. The basic a parameter would be 5.32 Å, but the structure would be modulated periodically in the a direction, with a "wavelength" of 41.5 Å. No change in this superlattice integral value has been observed between different crystals of the mineral under X-ray investigation, or by selected area electron diffraction.

A series of closely spaced spots parallel to c^* are also visible in the zero level a^* c^* net (Cu radiation) of Figure 4. Again, they may indicate a larger superlattice parameter in the c direction, with $c=7.277\times43.66$ Å. However, these multiple spots are not observed in other photographs involving c^*, due either to the poorer resolution of the Mo radiation used, or to the masking effect of the features described below. Unfortunately it was also impossible to confirm the multiplicity along c^* by electron diffraction due to the preferential alignment of crystallites on sample grids parallel to the perfect cleavage (001). (2) It is immediately noticeable that, whilst certain reflections are sharp, others are elongated, in varying degrees, parallel to c^*. On the basis of the extent of the elongation, the reflections can be subdivided into three types:

1. Sharp reflections: these occur only when:

$$h = 0 \quad \text{for } (h0l)$$
$$k = 0 \quad \text{or } 6n \text{ for } (0kl)$$
$$h = 3n \quad \text{and } k = 3n \text{ for } (hkl)$$

2. Reflections elongated by $c^*/2$ along c^*: these occur when:

$$h \neq 0 \quad \text{for } (h0l)$$
$$h \neq 0 \quad \text{or } 3n, \text{ and } k = 3n \text{ for } (hkl)$$

3. Continuous streaks parallel to c^* of uniform intensity, except for the falling off of atomic scattering factor with increasing $\sin\theta/\lambda$. These occur when:

$$k \neq 0 \quad \text{or } 6n \text{ for } (0kl)$$
$$k \neq 3n \quad \text{for } (hkl)$$

From the evidence of elongation of reflections parallel to c^*, it seems that the serpentine layers making up the crystals are displaced relative to each other. The displacement would be in the order of $\pm a/3$ and $\pm b/3$. The probability of the stacking mistake, α, calculated from the integral breadths of the streaks parallel to c^* (using the formula $b=3\alpha/(4-3\alpha)$, after Rucklidge and Zussman (1965), where b is the integral breadth)

would be approximately $\alpha = 0.4$ for the a direction (where $b = 0.5$). It is more difficult to give a value to the breadth in the b direction, since the streaks are continuous; these, however, can be interpreted as resulting from random stacking of the layers, such that the probability of the stacking mistake, α, must equal or approach unity.

Similar streaking could also be caused by rotation of each successive layer relative to its neighbours. A $\pm 60°$ rotation of the layers would produce single crystal photographs comparable to those presented here. However, rotation of basic serpentine layers, should these be individually corrugated parallel to a, would cause corrugations to show up in other directions as well, and would also inhibit stacking along c with the repeat distance of 7.28 Å. On the other hand, it is possible that although the fundamental layers are individually rotated, the corrugations are always superimposed onto these layers in the same direction with respect to the crystal as a whole.

Electron Microscopy

An ethyl alcohol-based suspension of the finely ground serpentine was dispersed by vibrating ultrasonically for one minute. Drops of the liquid were then pipetted onto sample grids previously covered by 300 Å thick carbon substrates. The specimens were viewed with a Siemens Emiskop I electron microscope. The same specimens were used for selected-area electron diffraction.

The first sets of observations were made at 100 kV using a standard sample stage. It was found that the diffraction patterns obtained would disappear within one minute of exposure to the electron beam. However, a cold finger stage was subsequently inserted into the microscope, with the result that the particles could be viewed for five minutes or more without any apparent changes taking place.

At high magnifications the mineral exhibits two distinct morphologies, with a complete range of intermediate transitional morphologies between the two end types. These are illustrated in Figures 5 and 6. The original flakes, lying parallel to (001), are still apparent. A number of these, when viewed at high magnifications, show the flakes traversed by regularly spaced parallel lines, somewhat similar to the electron optical fringes recorded by Brindley, *et al.*, (1958) and others. The separation of these parallel lines is in the order of 160 Å, which seems to bear a four-fold relationship to the superlattice parameter $a = 41.5$ Å recorded by X-ray diffraction.

In many cases the plates are clearly seen to be composed of a series of layers; each layer is made up of parallel-lying elongated laths. By observing the orientation of these component laths, one can deduce that

each layer is rotated with respect to its neighbours above and below. The layers break up at the edges into their constituent laths; the latter are scattered throughout the field of view. In turn, these laths show a ten-

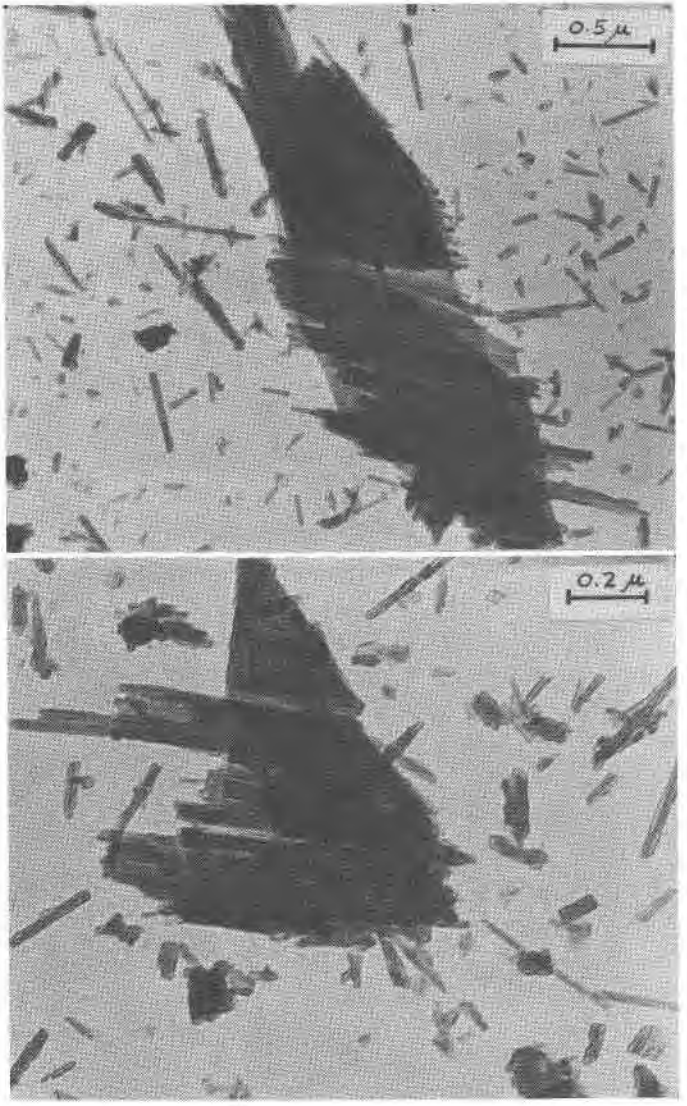

FIG. 5. (a) and (b). Electron micrographs of serpentine mineral, showing rotated superimposition of flakes, parallel arrangement of laths within flakes, laths with crinkled edges, and hollow tubes.

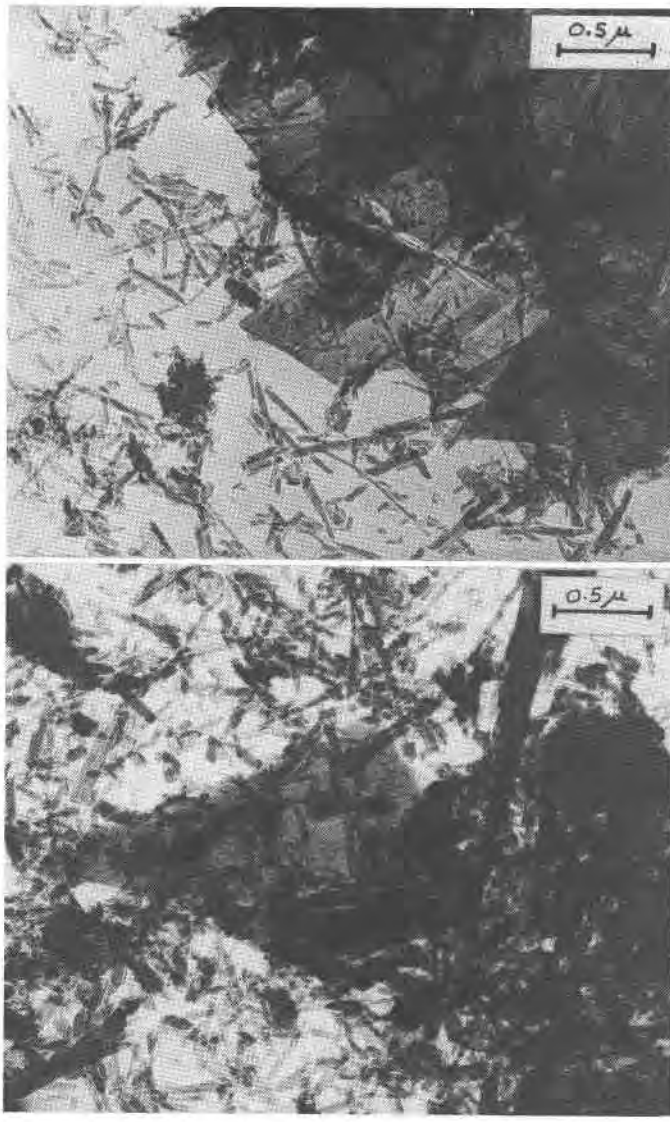

FIG. 6. (a) and (b). Electron micrographs of serpentine mineral, showing flakes with parallel striations, laths, and hollow tubes.

dency to curl up about an axis parallel to their length. Some of them exhibit this tendency in its initial stage, giving rise to crinkled edges. Other laths have gone a stage further, producing a close approximation

to chrysotile tubes. In a few examples, end on views of these "tubes" are visible, showing their hollow axes. The external diameter of these tubes can vary from 150 Å to 250 Å.

Electron Diffraction

Plates of the serpentine are always found to be lying parallel to the (001) cleavage. These give a well oriented a^* b^* net (Fig. 7a), showing the superlattice-controlled clustering of spots parallel to a^*, around certain multiple values of h. In all cases the latter is an integral multiple of 8, suggesting a superlattice parameter of 8×5.32 Å $= 41.5$ Å.

The process of transformation from plates to tubes can also be followed by selected area electron diffraction. Whereas the plates give diffraction patterns as described above, those of the laths and tubes show that considerable curvature has taken place. The resultant patterns are similar to the rotation photographs obtained from chrysotile tubes, both as bundles of fibres in X-ray diffraction, and as single tubes in electron diffraction. Difficulties were encountered in trying to record diffraction patterns from single fibres; the microscope was not equipped with a beam stop, so that the main beam generally blacked out the faint patterns given by the fibres. An example of patterns obtained is shown in Figure 7b. Reflections fall along lines perpendicular to the tube axes. The repeat distance between these layers is 5.32 Å. As in chrysotile, the zero layer contains both $00l$ and $0k0$ spots, while the first layer shows the characteristic flared spots indexed as (hkO). Similarly, the second layer contains $20l$ spots, and the third layer the flared spots (310) and (330). The laths have therefore have been curved about the x axis, and now give a pattern which approximates an electron diffraction pattern of chrysotile.

Discussion

The mineral described above has many of the properties characteristic of the serpentine group of minerals. However, the combination of these properties cannot be matched to any one of the known serpentine polymorphs alone, as discussed below. There are two possible explanations for the diversity of properties exhibited: this mineral could be an intimately compounded mixture of two or more other serpentine polymorphs, or it could be a new serpentine polymorph.

The morphology of the mineral is unusual for any serpentine. Single crystal plates 5 mm across have not been reported before, except possibly in the rare case of the lizardite from Kennack Cove (Midgley, 1951). Polysynthetic twinning is also rare in serpentines; it is found only

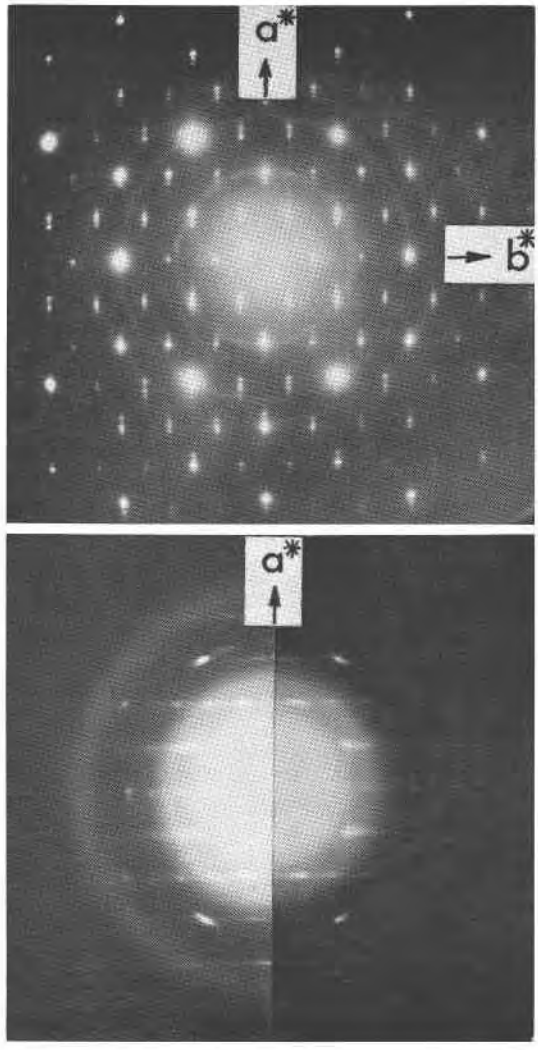

FIG. 7. (a) Electron diffraction pattern (a^* b^*) of serpentine mineral, showing superlattice-controlled clustering of spots parallel to a^*.

(b) Electron diffraction pattern of lath curved about an axis parallel to its length (a^*).

occasionally in antigorites. The refractive indices are low, even for chrysotile, whilst the centered biaxial negative interference figure is more in keeping with antigorite, although the optic angle is too large (2Vfor antigorite being 37°–61°).

Chemical analyses are never too conclusive in the identification of the

serpentine polymorphs. However, the author has plotted some 200 analyses from the literature on triangular diagrams: these show diffuse compositional zones for chrysotile, lizardite and antigorite. The mineral from the Tilley Foster Mine falls in the chrysotile zone. The analysis shows a small replacement of silicon by aluminum. Since the sample is known to be free from magnetite, one can also assume that magnesium is being replaced to a small extent by ferrous and ferric iron. However, more replacement, especially of Si by Al, would have been expected to have taken place in order to account for the large platy habit of the mineral. The corrugation of the sheets will reduce the necessity of Si replacement to alleviate mismatching of the layers. The Si:Mg ratio, higher than that required for the ideal serpentine composition, is also in keeping with corrugated sheets. However, once the crystals are broken down to dimensions small enough to reduce the effectiveness of the corrugations, they would be expected, and are indeed observed, to curl.

Thermal analyses, together with the destruction of the crystallinity by 1 N hydrochloric acid and by an electron beam, suggest similarities with chrysotile. However, no serpentine polymorph has yet been reported to produce protoenstatite on heating, either as a major or minor phase.

X-ray diffractograms, were it not for two weak and almost overlooked superlattice lines, would identify the mineral conclusively to be clino-chrysotile. However, single crystal photographs exclude this possibility. Without supporting evidence from electron diffraction, it is not possible to confirm the superlattice along c detected on precession photography. However, a six-layered cell would comply with the other observations of displacement or rotation of individual layers. Hence it is suggested that the mineral is a monoclinic six-layer serpentine ($c = 7.277 \times 6 = 43.66$ Å); it has a β angle approximating that of clino-chrysotile, having individual fundamental layers modulated periodically in the a direction of the crystal. These photographs show that there are stacking errors between successive layers, either as displacements of $\pm a/3$ and $\pm b/3$, or 60° rotation of the layers, or both. The electron micrographs suggest that both types of stacking errors may exist.

The regularly spaced parallel lines observed at high magnifications on the plates (Fig. 6b) are not believed to be electron optical fringes; they are rather corrugations of the plates showing incipient parting. Some of the bright lines visible parallel to the axes of the rods could be Fresnel fringes, obtained under slightly out of focus conditions, rather than hollow tubes. However, in many instances they are definitely tubular, with end sections visible, giving the rotation-type electron diffraction patterns generally associated with chrysotiles.

The transition from plates to tubes, as followed on the electron micro-

scope, is also unique. The plates have many of the characteristics of antigorite, whilst the tubes approximate chrysotile very closely. It is possible that the plates part along the junctions between adjacent alternating structural waves; these would then be free to curl into tubes.

A polymorphic mixture would offer a second explanation for the electron microscope observations: rather than being observations of different stages in the metamorphosis from an unstable platy, to a stable tubular crystal, the photomicrographs and diffraction patterns would be explained as being from stable material originally present in, and later released from, the macrocrystals. However, with the assumption that the dispersed state contains such a free mixture, one has then to explain why no such "mixture effect" shows up in the thermal analyses and powder diffractograms. One may also expect the complicated single crystal photographs, if mixture controlled, to vary from crystal to crystal, with different relative proportions of the constituents occurring in different crystals; the photographs are not found to vary, indicating either a remarkably constant mixture, which is unlikely, or a different polymorph altogether.

A number of other properties cannot be controlled or explained by the mixing of polymorphs. For example, the refractive indices of the macrocrystals are lower than those of any of the components of a possible mixture.

Conclusions

The mineral from the Tilly Foster Mine is believed to be an unstable polymorph of the serpentine group of minerals. Its unit cell is made up of six superimposed fundamental serpentine layers, with each successive layer displaced relative to its neighbours by $\pm a/3$ and $\pm b/3$, and, or by a rotation of $\pm 60°$. Individual layers are further modulated periodically in the a crystal direction. The stacking errors and layer modulations result in a crystal with superlattice-controlled a and c parameters.

The configuration described is stable only in its original macrocrystalline state, tending to break down into smaller, simpler units if assisted mechanically. Hence the finer fractions of a powdered specimen show that the crystals break up in stages, at first forming thin corrugated plates. The latter, in turn, part along weak corrugation joints, giving rise to rods which will necessarily be under strain due to the fundamental mismatching of the constituent silica tetrahedral and brucite octahedral layers. Unable to take up the strain in other ways, the rods resort to curling parallel to their elongation, as demonstrated in electron micrographs, finally producing chrysotile-like tubes.

ACKNOWLEDGEMENTS

The author is indebted to Dr. J. Zussman of the Department of Geology and Mineralogy, University of Oxford, for his valuable comments and for critically reading a preliminary draft of the manuscript.

Thanks are also due to Dr. J. A. V. Douglas, Miss C. M. Hunt, Mr. R. N. Delabio, and Mr. J. L. Bouvier, of the Geological Survey of Canada, Ottawa, and Miss J. Ng Yelim, Mr. R. Lake, and Mr. J. R. Rowland of the Mines Branch, Ottawa for their technical cooperation.

The loan of a Buerger precession camera from the Department of Geology, Dalhousie University, is also gratefully acknowledged.

REFERENCES

BRINDLEY, G. W., J. J. COMER, R. UYEDA, and J. ZUSSMAN (1958) Electron-optical observations with crystals of antigorite. *Acta Crystallogr.* **11,** 99–102

JAMBOR, J. L. AND C. H. SMITH (1964) Olivine composition detremination with small-diameter X-ray powder cameras. *Mineral Mag.* **33,** 730–741.

MIDGLEY, H. G. (1951) A serpentine mineral from Kennack Cove, Lizard, Cornwall. *Mineral Mag.* 29, 526–530

RUCKLIDGE, J. C. AND J. ZUSSMAN (1965) The crystal structure of the serpentine mineral, lizardite $Mg_3Si_2O_5(OH)_4$. *Acta Crystallogr.* **19,** 381–389

Manuscript received, December 17, 1966; accepted for publication, July 17, 1967.